TIFR/TH/96-58
hep-ph/yymmnn

Constraints on the Charged Higgs Sector from the Tevatron Collider Data on Top Quark Decay

Monoranjan Guchait[1] and D.P. Roy[2]

Theoretical Physics Group
Tata Institute of Fundamental Research
Homi Bhabha Road, Mumbai 400 005, India

Abstract

The top quark data in the lepton plus τ channel offers a viable probe for the charged Higgs boson signal. We analyse the recent Tevatron collider data in this channel to obtain a significant limit on the $H^{\pm}$ mass in the large $\tan\beta$ region.

Pacs Nos: 11.30.Pb,13.35.Dx,14.65.Ha

[1]e-mail:guchait@@theory.tifr.res.in
[2]e-mail:dproy@@theory.tifr.res.in

The discovery of the top quark signal at the Tevatron collider [1,2] has generated a good deal of current interest in the search of new particles in top quark decay. The large mass of top offers the possibility of carrying on this search to a hitherto unexplored mass range for these particles. In particular the top quark decay is known to provide by far the best discovery limit for one such new particle, i.e. the charged Higgs boson [3] of the minimal supersymmetric standard model (MSSM). The signature of the charged Higgs boson in top quark decay is based on its preferential coupling to the τ channel in contrast to the universal W boson coupling. Thus a departure from the universality prediction can be used to separate the charged Higgs boson signal from the W background in

$$t \to bH(bW) \to b\tau\nu. \tag{1}$$

In particular, the top quark decay into the τ lepton channel provides a promising signature for charged Higgs boson in the region

$$\tan\beta \gtrsim m_t/m_b, \tag{2}$$

where $\tan\beta$ denotes the ratio of the vacuum expectation values of the two Higgs doublets in MSSM.

In this note we shall analyse the recent CDF data on $t\bar{t}$ decay events in the $\ell\tau$ channel, where ℓ denotes e and μ [2,4,5]. This channel has the advantage of a low background. As we shall see below, the number of $t\bar{t}$ events in this dilepton channel relative to the ℓ + multijet channel gives a significant lower bound on the $H^\pm$ mass in the large $\tan\beta$ region (2).

In the diagonal KM matrix approximation, the charged Higgs boson couplings to the fermions are given by

$$\mathcal{L} = \frac{g}{\sqrt{2}m_W} H^+ \left\{\cot\beta m_{ui}\bar{u}_i d_{iL} + \tan\beta m_{di}\bar{u}_i d_{iR} + \tan\beta m_{\ell i}\bar{\nu}_i \ell_{iR}\right\} + \text{h.c.} \tag{3}$$

where the subscript i denotes quark and lepton generation. The leading log QCD correction is taken into account by substituting the quark mass parameters by their running masses evaluated at the $H^\pm$ mass scale [6]. The resulting decay widths are

$$\begin{aligned}\Gamma_{t\to bW} &= \frac{g^2}{64\pi m_W^2 m_t}\lambda^{\frac{1}{2}}\left(1, \frac{m_b^2}{m_t^2}, \frac{m_W^2}{m_t^2}\right) \\ &\quad \left[m_W^2(m_t^2+m_b^2) + (m_t^2-m_b^2)^2 - 2m_W^4\right]\end{aligned} \tag{4}$$

$$\begin{aligned}\Gamma_{t\to bH} &= \frac{g^2}{64\pi m_W^2 m_t}\lambda^{\frac{1}{2}}\left(1, \frac{m_b^2}{m_t^2}, \frac{m_H^2}{m_t^2}\right) \\ &\quad \left[(m_t^2\cot^2\beta + m_b^2\tan^2\beta)(m_t^2+m_b^2-m_H^2) - 4m_t^2 m_b^2\right]\end{aligned} \tag{5}$$

$$\Gamma_{H\to\tau\nu} = \frac{g^2 m_H}{32\pi m_W^2} m_\tau^2 \tan^2\beta \tag{6}$$

$$\Gamma_{H\to c\bar{s}} = \frac{3g^2 m_H}{32\pi m_W^2}(m_c^2 \cot^2\beta + m_s^2 \tan^2\beta). \tag{7}$$

They clearly show a large branching fraction for $t \to bH$ decay at $\tan\beta \lesssim 1$ and $\tan\beta \gtrsim m_t/m_b$, while the branching fraction for $H \to \tau\nu$ decay is $\simeq 1$ at $\tan\beta \gg 1$. Thus one expects a large charged Higgs boson signal in top quark decay into the τ channel (1) in the large $\tan\beta$ region (2).

In the present analysis, we shall concentrate in the $\tan\beta \gg 1$ region, for which the charged Higgs boson decays dominantly into $\tau\nu$. The basic process of interest is $t\bar{t}$ production via quark-antiquark (or gluon-gluon) fusion, followed by their decays into charged Higgs or W boson channels, i.e.

$$q\bar{q} \to t\bar{t} \to b\bar{b}(W^+W^-, W^\pm H^\mp, H^+H^-). \tag{8}$$

The most important $t\bar{t}$ signal is observed in the ℓ + multijet channel [1,2]. It comes from the W^+W^- final state with a branching fraction of 24/81. The corresponding branching fraction from this final state into the $\ell\tau$ channel is only 4/81. However there would be an additional contribution to the $\ell\tau$ channel from the $W^\pm H^\mp$ final state with a large branching fraction of 4/9, which is to be weighted of course by the ratio $\Gamma_{t\to bH}/\Gamma_{t\to bW}$. Thus a comparison of the number of $t\bar{t}$ events in the two channels leads to an upper limit on this ratio, which can be translated into lower limit on $H^\pm$ mass for a given $\tan\beta$.

For a quantitative estimate of the above limit, we have to consider the various kinematic cuts and detection efficiencies [2,5]. Our analysis is based on a parton level Monte Carlo simulation of $t\bar{t}$ production using the quark and gluon structure functions of [7]. This is followed by the decays

$$t \xrightarrow{W^+} b\ell\nu,\ \bar{t} \xrightarrow{W^-} \bar{b}q\bar{q}' \tag{9}$$

and vice versa for the ℓ + multijet channel. The quark jets are merged according to the CDF jet cone algorithm of $\Delta R = (|\Delta\eta|^2 + |\Delta\phi|^2)^{1/2} = 0.7$. The resulting final state is required to satisfy the CDF cuts [2]

$$p_T^\ell > 20 \text{ GeV},\ |\eta_\ell| < 1,\ \not{E}_T > 20 \text{ GeV and } n_{\rm jet} \geq 3 \text{ (with } E_T^j > 15 \text{ GeV},\ |\eta_j| < 2). \tag{10}$$

We estimate the efficiency factor for these kinematic and topological cuts to be 52% for $m_t = 175$ GeV. This has to be supplemented by the following CDF efficiency factors [2,5,8];

$$\epsilon_{tr}^\ell = .93,\ \epsilon_{id}^\ell = .87,\ \epsilon_{iso}^\ell = .9,\ \epsilon_b = .4,\ \epsilon_{az} = .85, \tag{11}$$

corresponding to lepton triggering, identification and isolation-cut along with those due to SVX b-tagging and azimuthal gaps in the detector. The combined efficiency factor is 12.8%, in reasonable agreement with the CDF estimate of 11.8% [2] including hadronisation and a more exact detector simulation.

The measured $\bar{t}t$ cross-section from this channel, including SLT b-tagging, is [2]

$$\sigma_t = 7.5 \pm 1.5\ pb. \tag{12}$$

This is 40-50% higher than the NLO QCD prediction for $m_t = 175$ GeV [9]. We shall use this cross-section for normalisation. Thus our results will be independent of any theoretical

model for the $\bar{t}t$ cross-section. It will only depend on the preferencial $H^{\pm}$ coupling to the τ channel vis-a-vis the universal $W^{\pm}$ boson coupling. It should be noted here that the above cross-section corresponds to the WW contribution to the $\bar{t}t$ cross-section, represented by the 1st term of (8), since any contribution from the other terms would have very small detection efficiency for this channel.

The $\ell\tau$ channel of our interest corresponds to the decays

$$t \xrightarrow{W^+} b\ell\nu,\ \bar{t} \xrightarrow{W^-(H^-)} \bar{b}\tau\nu \tag{13}$$

and vice versa, where the τ lepton coming from $W(H)$ decay has a definite polarization $P_\tau = -1(+1)$. It is identified in its hadronic decay mode as a thin jet containing 1 or 3 charged prongs [4,5]. This accounts for a τ branching fraction of about 64% [10]. The dominant contributions come from

$$\tau \to \pi\nu(12\%),\ \rho\nu(25\%),\ a_1\nu(15\%), \tag{14}$$

adding up to a little over 80% of the hadronic τ decay. We shall combine these three decay modes and scale up their sum by 20% to simulate hadronic τ-decay. The decay distributions are simply given by [11]

$$\frac{d\Gamma_\pi}{\Gamma_\pi d\cos\theta} = \frac{1}{2}(1 + P_\tau \cos\theta), \tag{15}$$

$$\frac{d\Gamma_v}{\Gamma_v d\cos\theta} = \frac{1}{2}\left(1 + \frac{m_\tau^2 - 2m_v^2}{m_\tau^2 + 2m_v^2} P_\tau \cos\theta\right),\ v = \rho, a_1 \tag{16}$$

where θ is the direction of the decay hadron in τ rest frame relative to the τ line of flight. It is related to the fraction x of τ momentum carried by the hadron,

$$\cos\theta = \frac{2x - 1 - m_\pi^2, v/m_\tau^2}{1 - m_\pi^2, v/m_\tau^2}. \tag{17}$$

This decay hadron momentum is refered to below as p^τ.

The resulting final state is required to satisfy the CDF kinematic cuts [4,5],

$$p_T^\ell > 20\ \text{GeV},\ |\eta_\ell| < 1,\ p_T^\tau > 15\ \text{GeV},\ |\eta_\tau| < 1.2. \tag{18}$$

The corresponding efficiency factors are shown in the first column of Table 1 for the WW and WH contributions with different charged Higgs boson masses. It includes the hadronic branching fraction of τ along with a factor of 0.8 due to azimuthal gaps in the detector, resulting in 15% (5%) loss to $\ell(\tau)$ detection efficiency [8]. The opposite polarizations of τ coming from W and H decays results in a somewhat larger efficiency factor for the latter, which increases further with increasing H mass. The second column shows the CDF efficiency factors for the lepton trigger, isolation and idendification as well as the τ identification. These are expected to be essentially process independent. The last column shows the efficiency factors for the topological and missing-E_T cuts [4,5]

$$n_{\text{jet}} \geq 2\ (\text{with}\ E_T^j > 10\ \text{GeV},\ |\eta_j| < 2), \tag{19}$$

$$H = p_T^\ell + p_T^\tau + \not{E}_T + \sum_j E_T^j > 180 \text{ GeV}, \tag{20}$$

$$\sigma_{\not{E}_T} = \not{E}_T / \sqrt{p_T^\ell + p_T^\tau + \sum_j E_T^j} > 3 \text{ GeV}^{1/2}. \tag{21}$$

For the WW contribution, the efficiency factors for the kinematic and topological cuts from the CDF simulation [5] are shown in parantheses for comparison. For both cases they are 15-20% below our MC estimates, which indicate an overall error of $\sim 30\%$ in our MC result.

The product of the efficiency factors in the three columns of Table 1 gives the overall acceptance factor for the $\ell\tau$ channel. This is to be multiplied by the branching fraction of 4/81 for the WW contribution and 4/9 times $\Gamma_{t\to bH}/\Gamma_{t\to bW}$ for the WH. The resulting factor gives the corresponding $\ell\tau$ cross-section as a fraction of the σ_t of (12).

Fig. 1 shows the predicted cross-section in the $\ell\tau$ channel against $\tan\beta$ for several charged Higgs boson masses. The scale on the right shows the corresponding number of events for the accumulated CDF luminosity of 110 fb^{-1}. The prediction includes the WW contribution of 14 fb, i.e. 1.5 events. The corresponding number from the CDF simulation is 1.2 events [5,8]. It may be noted that the dominant contribution comes from WW for $\tan\beta = 5 - 10$, where $t \to bH$ width has a pronounced dip. However the WW is overwhelmed by the WH contribution, when kinematically allowed, for $\tan\beta \gtrsim m_t/m_b$. The preliminary CDF data shows 4 events in this channel against a background of 2 ± 0.4 [2,4,5]. The corresponding 95% CL limit of 7.7 events [10,12] is indicated in the figure. This implies a $H^\pm$ mass limit of 100 GeV for $\tan\beta \geq 40$, going up to 120 GeV for $\tan\beta \geq 50$. One may scale down the predicted cross-section by 30% to account for the difference between the acceptance factors of CDF simulation and ours. This would correspond to an upward shift of the above $\tan\beta$ limit by about 10 units for a given $H^\pm$ mass. Nonetheless it would still represent a very significant constraint on the charged Higgs boson mass in the large $\tan\beta$ region.

The mass limits of Fig. 1 for different values of $\tan\beta$ are converted into a 95% exclusion contour in the $m_H - \tan\beta$ plane in Fig. 2. As mentioned above, a 30% reduction in the signal cross-section would correspond to a rightward shift of this contour by roughly 10 units in $\tan\beta$. The scale on the right shows the corresponding pseudo-scalar Higgs mass m_A from the MSSM mass relation, $m_{H^\pm}^2 - m_A^2 = m_W^2$, at the tree level [13]. The radiative correction to this mass relation is known to be no more than a few GeV. One sees from this figure that a relatively light pseudo-scalar mass ($m_A \leq 60$ GeV) is disallowed for $\tan\beta \geq 40$. It is precisely in this region of m_A and $\tan\beta$ that one expects to get a significant radiative correction to R_b ($\Gamma_z^b/\Gamma_z^{\rm had}$) from the Higgs sector of MSSM [14]. Thus the so called large $\tan\beta$ solution to the (so called!) R_b anomaly seems to be strongly disfavoured by the above CDF data.

Recently the CDF collaboration has obtained a limit on the charged Higgs mass in the large $\tan\beta$ region [15] on the basis of their analogous data in the inclusive τ channel. Thus it is instructive to compare the relative merits of the two channels for probing the charged Higgs signal. The inclusive τ channel corresponds to a larger branching fraction than the $\ell\tau$ channel analysed here. However it is compensated by much stronger experimental cuts, required to control the background. Consequently the final signal cross-section in the inclusive τ channel is similar to that in the $\ell\tau$ channel. This can be seen by comparing the predicted cross-sections in the two channels in the region of $\tan\beta = 5 - 10$. The reason we get a much

larger signal cross-section in the large $\tan\beta$ region compared to [15] and hence a stronger mass limit is due to the different normalisation procedure followed in the two cases. We use the $t\bar{t}$ cross-section in the WW decay mode as measured via the lepton plus ≥ 3 jets channel for our normalisation, while the QCD prediction for the inclusive $t\bar{t}$ cross-section is used for normalisation in [15]. The former method is evidently more powerful in the large $\tan\beta$ region and should be used in the analysis of the inclusive τ channel as well.

It should be noted here that even with stronger cuts the number of estimated background events in the inclusive τ channel are 5 times larger than in the $\ell\tau$ channel, for equal luminosity [5,15]. Thus the $\ell\tau$ channel will be clearly more advantageous at Tevatron upgrade, which promises a 20 times higher luminosity along with a 2 times larger $t\bar{t}$ cross-section. In particular the $\ell\tau$ channel with b-tagging seems to be practically free from non-top background [4,5]. The main background in this case is from the $t\bar{t}$ decay via the WW mode. This can be suppressed relative to the $H^{\pm}$ signal by exploiting the opposite polarizations of τ lepton in the two cases [16]. Thus the $\ell\tau$ channel with b-tagging is best suited for the charged Higgs boson search at the Tevatron upgrade as well as the LHC.

In summary, the $t\bar{t}$ data in the $\ell\tau$ channel is well suited to probe for a charged Higgs boson signal because of the small background. On the basis of the recent CDF data in this channel we can already get a significant limit on the $H^{\pm}$ mass in the large $\tan\beta$ region. With a much higher luminosity expected at the Tevatron upgrade the probe can be extended over a significantly wider range of $H^{\pm}$ mass and $\tan\beta$.

It is a pleasure to thank Prof. M. Hohlmann of the CDF collaboration and Prof. N.K. Mondal of D$\emptyset$ for many helpful discussions.

References

1. CDF Collaboration: F. Abe et. al., Phys. Rev. Lett. 74, 2626 (1995);
   DØ Collaboration: S. Abachi et. al., Phys. Rev. Lett. 74, 2632 (1995).

2. P. Tipton, 28th Intl. Conf. on High Energy Physics, Warsaw (1996).

3. V. Barger and R.J.N. Phillips, Phys. Rev. D41, 884 (1990);
   A.C. Bawa, C.S. Kim and A.D. Martin, Z. Phys. C47, 75 (1990);
   R.M. Godbole and D.P. Roy, Phys. Rev. D43, 3640 (1991);
   R.M. Barnett, R. Cruz, J.F. Gunion and B. Hubbard, Phys. Rev. D47, 1048 (1993).

4. CDF Collaboration: S. Leone, XI Topical Workshop on $\bar{p}p$ Collider Physics, Padova (1996), Fermilab-Conf. 96/195-E.

5. CDF Collaboration: M. Hohlmann, Lake Louise Winter School (1996).

6. M. Drees and D.P. Roy, Phys. Lett. B269, 155 (1991);
   D.P. Roy, ibid B283, 403 (1992).

7. A.D. Martin, R.G. Roberts and W.J. Stirling, Phy. Lett. B306, 145 (1993) and B309, 492 (1993).

8. M. Hohlmann, Private Communication.

9. E. Berger and H. Contoparagos, Phys. Lett. B361, 115 (1995);
   S. Catani et. al., hep-ph/9602208 (1996).

10. Particle Data Group: R. M. Barnett et al, Phys. Rev. D54, 1 (1996).

11. B.K. Bullock, K. Hagiwara and A.D. Martin, Phys. Rev. Lett. 67, 3055 (1991);
    D.P. Roy, Phys. Lett. B277, 183 (1992).

12. O. Helene, Nucl. Inst. and Meth., 212, 319 (1983).

13. J.F. Gunion, H.E. Haber, G. Kane and S. Dawson, The Higgs Hunters' Guide, Addison Wesley, Reading, MA (1990).

14. D. Garcia, R. Jimenez and J. Sola, Phys. Lett. B347, 321 (1995);
    P.H. Chankowski and S. Pokarski, Nucl. Phys. B (to be published).

15. CDF Collaboration: C. Loomis, DPF meeting, Minneapolis (1996).

16. S. Raychaudhuri and D.P. Roy, Phys. Rev. D52, 1556 (1995) and D53, 4902 (1996).

Table 1: The efficiency factors for the $\ell\tau$ channel corresponding to the indicated kinematical and topological cuts. For the WW process, the corresponding efficiencies from the CDF simulation are shown in parenthesis. The middle column shows the triggering, isolation and identification efficiencies from the CDF simulation.

Eff. Process	$p_T^{\ell,\tau}$ & geom.	$\epsilon^{\ell}_{tr}, \epsilon^{\ell}_{iso}$, ϵ^{ℓ}_{id}, ϵ^{τ}_{id}	jets, H_T & $\not\!\!E_T$
WW	.16 (.13)	.93 × .9	.64 (.54)
$WH(80)$	.19	× .87 × .5	.61
$WH(100)$	.21	= .36	.62
$WH(120)$	.22		.64
$WH(140)$	.22		.65

Figure Captions

Fig.1 : The predicted cross-section (No. of events) shown against $tan\beta$ for different $H^{\pm}$ masses. The 95% C.L limit corresponding to 7.7 events is shown as a dashed line.

Fig.2 : The 95% C.L exclusion contour in the $H^{\pm}$ mass and $tan\beta$ plane. The corresponding pseudoscalar mass m_A is indicated on the right.

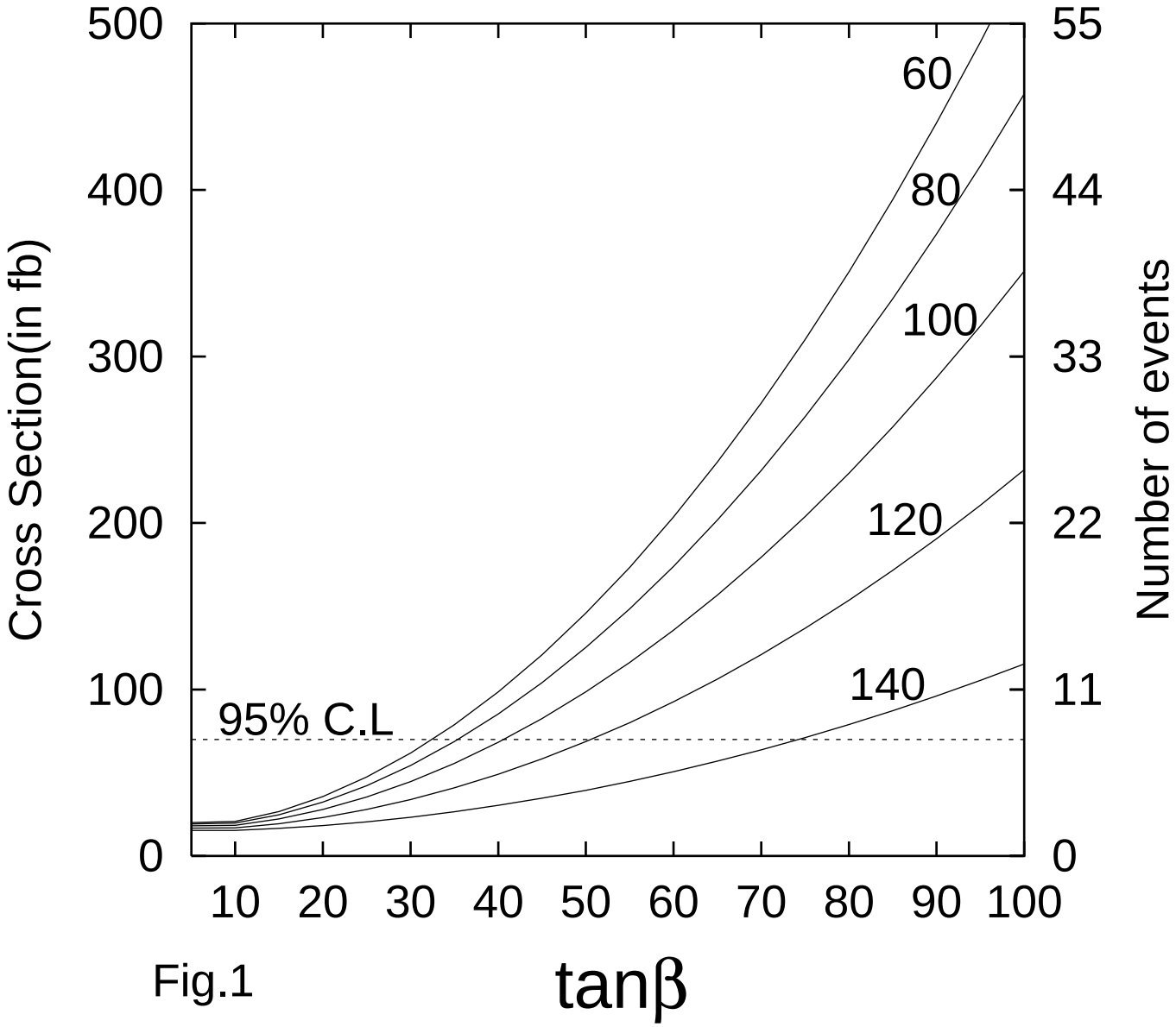
500
400
300
200
100
0
55
44
33
22
11
0
Cross Section(in fb)
Number of events
60
80
100
120
140
95% C.L
10
20
30
40
50
60
70
80
90
100
tanβ

Fig.1

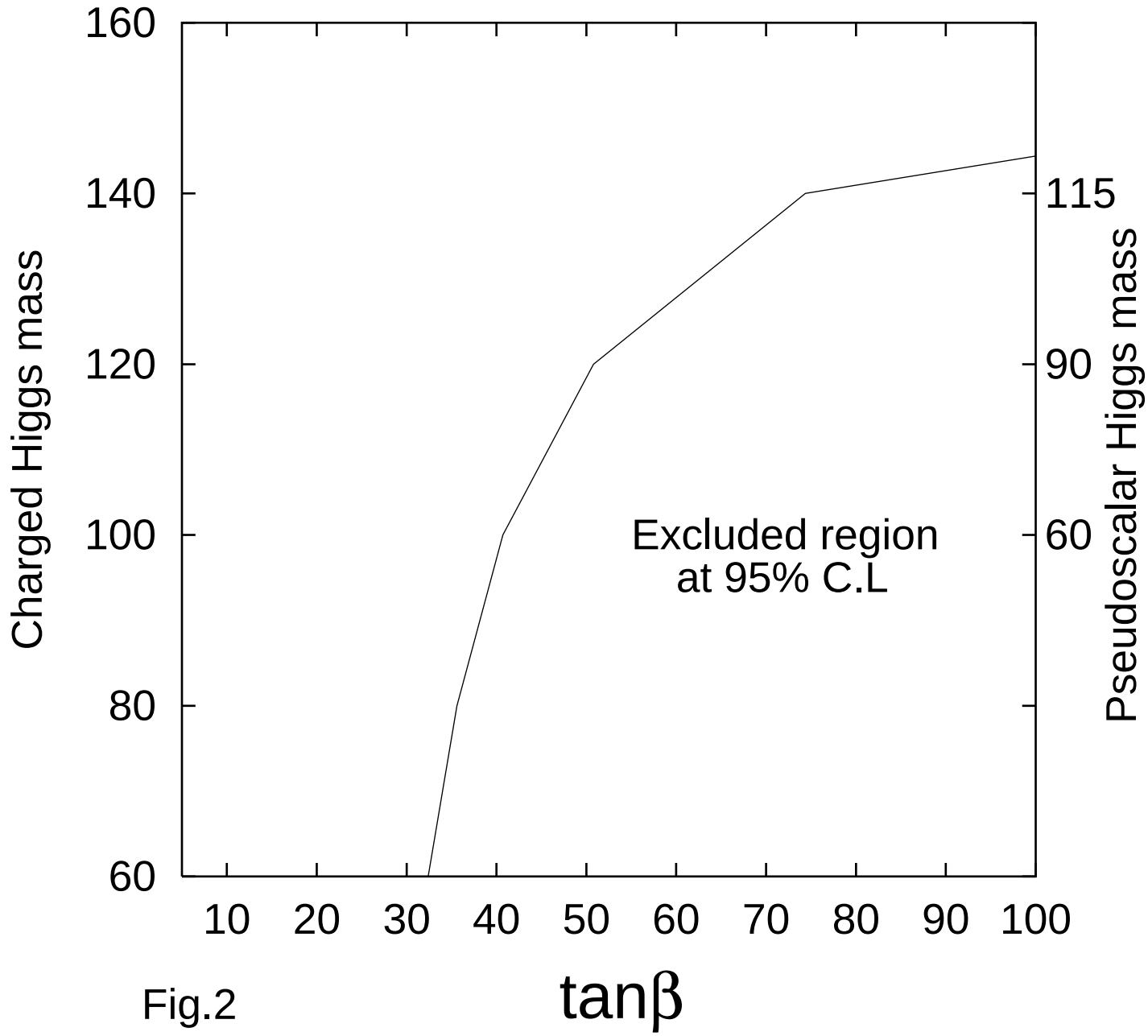
160
140
120
100
80
60
Charged Higgs mass
115
90
60
Pseudoscalar Higgs mass
Excluded region
at 95% C.L
10
20
30
40
50
60
70
80
90
100
tanβ

Fig.2